

1 **Measurement report: Ambient volatile organic compounds (VOCs) pollution at urban**
2 **Beijing: characteristics, sources, and implications for pollution control**

3 Lulu Cui¹, Di Wu¹, Shuxiao Wang^{1,2*}, Qingcheng Xu¹, Ruolan Hu¹, Jiming Hao^{1,2}

4 ¹*State Key Joint Laboratory of Environment Simulation and Pollution Control, School of Environment,*

5 *Tsinghua University, Beijing 100084, China*

6 ²*State Environmental Protection Key Laboratory of Sources and Control of Air Pollution Complex, Beijing*

7 *100084, China*

8 * Corresponding author. E-mail address: shxwang@tsinghua.edu.cn

9 **Abstract**

10 The increasing ozone (O_3) pollution and high fraction of secondary organic aerosols (SOA) in fine particle mass
11 highlighted the importance of volatile organic compounds (VOCs) in air pollution control. In this work, four
12 intensive field measurements of VOCs during winter of 2018 (from 1 December of 2018 to 17 January of 2019),
13 spring (15 April to 27 May), summer (17 June to 13 July) and autumn (22 September to 27 November) of 2019
14 were conducted at an urban site in Beijing a campaign of comprehensive field observations was conducted at an
15 urban site in Beijing, from December 2018 to November 2019, to characterize VOCs sources and their
16 contributions to air pollution. The total mixing ratio of the 95 quantified VOCs (TVOC) observed in this study
17 ranged from 5.5–118.7 ppbv with the mean value of 34.9 ppbv. Alkanes, OVOCs and halocarbons were the
18 dominant chemical groups, accounting for 75–81% of the TVOCs across the sampling months. The molar ratios
19 of VOCs to NO_x indicated that O_3 formation was limited by VOCs during the whole sampling period. Positive
20 matrix factorization (PMF) analysis showed that diesel vehicle exhaust, gasoline vehicle exhaust and industrial
21 emissions were the main VOCs sources during both the O_3 -polluted and $PM_{2.5}$ -polluted months. On the base of
22 O_3 formation impact, VOCs from fuel evaporation and diesel exhaust particularly toluene, xylenes, trans-2-

23 butene, acrolein, methyl methacrylate, vinyl acetate, 1-butene and 1-hexene were the main contributors,
24 illustrating the necessity of conducting emission controls on these pollution sources and species for alleviating
25 O_3 pollution. Instead, VOCs from diesel exhaust and coal/biomass combustion were found to be the dominant
26 contributors for secondary organic aerosol formation potential (SOAFP), particularly the VOC species of toluene,
27 1-hexene, xylenes, ethylbenzene and styrene, and top priority should be given to these for the alleviation of haze
28 pollution. This study provides insights for government to formulate effective VOCs control measures for air
29 pollution in Beijing.

30 **Key words:** VOCs, OFP, SOAFP, Source appointment

31 **1. Introduction**

32 The ozone (O_3) and fine particulate matter ($PM_{2.5}$) pollution has restricted improvements in air quality in China.
33 Observation data from the Chinese Ministry of Environment and Eclogy (MEE) network has witnessed an upward
34 trend for O_3 across the country over the period 2013-2019 (Fu et al., 2019; Li et al., 2017; Li et al., 2020; Shen
35 et al., 2019; Fan et al., 2020). Besides, haze pollution occurred in urban sites in recent years were commonly
36 characterized by enhanced formation of secondary organic aerosols (SOA) in fine particles, e.g., the fraction of
37 SOA in organic aerosols reached 58% in Xi'an during winter 2018 and 53% in urban Beijing during winter
38 2014(Kuang et al., 2020; Li et al., 2017b; Sun et al., 2020; Xu et al., 2019). Volatile organic compounds (VOCs)
39 are key precursors for the formation of O_3 via gas-phase reactions (Odum et al., 1997; Atkinson, 2000; Sato et
40 al., 2010; Huang et al., 2014). In highly polluted urban regions, the O_3 formation was generally VOCs-limited,
41 and it is suggested that VOCs emission control is necessary for effective alleviation of photochemical smog (Liu
42 et al., 2020a,b; Shao et al., 2009; Wang et al., 2020; Xing et al., 2011). Besides, the VOCs compounds including
43 aromatics and biogenic species have significant impact on SOA formation which play an important role in haze
44 formation (Huang et al., 2014; Tong et al., 2021). VOCs emission abatement is therefore imperative for
45 improving air quality in China.

46 VOCs in ambient air can be emitted by a variety of sources including both anthropogenic and biogenic
47 sources. While biogenic emissions are significantly greater than anthropogenic emissions globally (Doumbia et
48 al., 2021; Sindelarova et al., 2022), anthropogenic emissions play the dominant role in urban and surrounding
49 areas (Warneke et al., 2007; Ahmad et al., 2017; Wu and Xie, 2018). The VOC observations in China showed
50 distinct differences in anthropogenic sources among different regions. For example, solvent use and vehicle
51 exhaust are primary VOCs sources in urban Shanghai and urban Guangzhou, while the primary sources of VOCs

52 in Wuhan, Zhengzhou and Beijing cities are combustion and vehicle exhaust (Han et al., 2020; Shen et al., 2020;
53 Liu et al., 2020a; Li et al., 2019a). Apart from the diversity of emission sources, different VOCs species exhibited
54 different propensities to form O_3 and SOA. Observation-based studies commonly applied the O_3 formation
55 potential (OFP) and SOA formation potential (SOAFP) scales to quantify the relative effects of specific VOCs
56 and sources on O_3 and SOA formation and to aid in the development of efficient control strategies (Carter and
57 Atkinson, 1989; Chang and Rudy, 1990; Han et al., 2020; Zhang et al., 2017). Although there have been many
58 studies on ambient VOCs in various locations (e.g., urban, rural, and industrial areas), most of these
59 measurements were confined to short periods (a few days or a certain season), and the understanding of temporal
60 variations of concentrations, sources as well as the influence of photochemical reactions of VOCs on annual scale
61 was still limited. Besides, most of the available reports on VOCs analysis based on online analytical techniques
62 include mainly non-methane hydrocarbon compounds, and thus the characteristics of VOCs as well as their
63 relationships with $PM_{2.5}$ and O_3 cannot be fully revealed since OVOC also participate actively in chemical
64 reactions related to secondary formation (Li et al., 2019a; Zhao et al., 2020; Yang et al., 2018; Sinha and Sinha.,
65 2019). Therefore, the long-term and comprehensive monitoring of VOCs are desired.

66 As the capital and one of the largest megacities in China, Beijing has been suffering from severe O_3 pollution
67 due to rapid economic development and increases in precursor emissions (Wang et al., 2014a; Wang et al., 2017;
68 Li et al., 2019d; Zhao et al., 2020). According to the Report on the State of the Ecology and Environment in
69 Beijing, the average 90th percentile O_3 daily maximum 8 h concentration in Beijing exceeded the national
70 standards, reaching 193, 192, and 191 $\mu g/m^3$ in 2017, 2018, and 2019, respectively. In addition, the number of
71 motor vehicles in Beijing reached 6.365 million at the end of 2019 (<http://beijing.gov.cn>), making Beijing the
72 top city in China in terms of number of motor vehicles. The existing field measurements in Beijing were mostly

73 conducted before 2016, and the observation in most recent years is quite limited (Li et al., 2015; Li et al., 2019c;
74 Liu et al., 2020a; Yang et al., 2018). In this work, ambient air samples were collected at an urban site in Beijing
75 from December 2018 to mid-January 2019, mid-April to late May 2019, mid-June to mid-July 2019, and late
76 September to late November 2019, respectively.a campaign of comprehensive field observations was conducted
77 at an urban site in Beijing during December 2018 and November 2019 for the analysis of VOCs. Several O₃ and
78 PM_{2.5} pollution events were captured during the sampling period. The characteristics and the contribution of
79 specific species and sources of VOCs on O₃ and SOA formation, with a focus on photochemical and haze
80 pollution periods, were analyzed in detail. The results and implications from this study can provide useful guidance
81 for policymakers to alleviate ozone and haze pollution in Beijing.

82 **2. Methodology**

83 **2.1 Field measurement**

84 The sampling site is at the roof of a three-floor building on the campus of Tsinghua University (40.00°N,
85 116.33°E), northwest of Beijing urban area (Fig. S1). The altitude of the sampling site is 57 m. This sampling
86 site is surrounded by school and there are no large emission sources nearby, therefore it can represent the urban
87 air quality in Beijing. Details of the site description is found in Xu et al., (2019).

88 The air samples were collected using 6 L summa canisters (Entech, USA) with a stable rate of 4.26 ml/min.
89 The samples were pre-processed to remove N₂, O₂, CO₂, CO and H₂O in the samples and to further concentrate
90 the samples in volume by the cryogenic pre-concentrator (Model 7100, Entech Instruments Inc., USA). Pressure
91 gage was used to test if the canister has air leakage exist before sampling every time, and blanks were prepared
92 using cleaned canisters to fill with high purity nitrogen. The cryotrap of precooling system was baked before
93 analyses each day and between every samples. The VOCs in air samples were analyzed by a gas chromatography

94 system that was equipped with a mass spectrometric detector (GC-MS) (Agilent Tech., 7890/5975, USA). The
95 suitabilityavailability of this system for VOCs measurement are well verified and it has been used in field
96 campaigns (Li et al., 2014; Wu et al., 2016). ~~The column temperature was controlled by an initial temperature of~~
97 ~~40 °C.~~ The ~~ovenprogrammed~~ temperature was ~~programmed at 40 °C for 3 minutes initially, then raised to used~~
98 ~~with helium as carrier gas, and the flow rate was set at 1.5 ml min⁻¹. The initial temperature was set at 90 °C at~~
99 ~~8°C per minute, and later raisedthen switched~~ to 220 °C ~~at 6°C per minute, holding for 9 minutes~~. In this work,
100 95 target VOCs, including 25 alkanes, 8 alkenes, 16 aromatics, 34 halocarbons and 12 OVOC were quantified.
101 It should be noted that VOCs compounds (C2-C3) with low boiling point (i.e., ethane, ethene, acetylene,
102 and propane) were not detected by the GC-MS system. The standard substance (SPECTRA GASES Inc., USA)
103 mentioned for Photochemical Assessment Monitoring Stations (PAMS) and US EPA TO-15 standard was used
104 to construct the calibration curves for the target VOCs. Quality assurance and quality control, including method
105 detection limit (MDL) of each compound, laboratory and field blanks, retention time, accuracy and duplicate
106 measurements of samples were performed according to USEPA Compendium Method TO-15 (USEPA 1999).
107 The correlated coefficients of the calibration curves for all the compounds were > 0.95. The relative standard
108 deviation (RSD) for all of compounds of triplicates were 0.5%-6.0%. Previous field measurements have
109 reported that the precision of GC-MS system for hydrocarbons and aldehydes was below 6% and 15%,
110 respectively (Li et al., 2014; Wu et al., 2016). In this work, one kind of aldehyde substance, i.e.,
111 acroleinethyleaerolein was detected, with R^2 and RSD of 0.99 and 4.5%, respectively.
112 During the sampling periods, the measurements of PM_{2.5}, gaseous pollutants (NO_x and O₃), and
113 meteorological variables (such as temperature, relative humidity, wind speed, and wind direction) were
114 conducted simultaneously. SO₂, NO_x and O₃ were analyzed using the the Pulsed Fluorescence SO₂ Analyzer

115 (Thermo Fisher Scientific USA, 43I), Chemiluminescence NO-NO₂-NO_x Analyzer (Thermo Fisher Scientific
116 USA, 17I) and ultra-violet (UV) photometric O₃ Ozone Analyzer (Thermo Fisher Scientific USA, 49I) and NO-
117 NO₂-NO_x Analyzer (Thermo Fisher Scientific USA, 17I), respectively. The mass concentration of PM_{2.5} was
118 measured using an oscillating balance analyzer (TH-2000Z, China) (Wang et al., 2014a). The quality assurance
119 of SO₂, NO₂, O₃, and PM_{2.5} was conducted based on HJ 630-2011 specifications. Meteorological variables
120 including wind speed (WS), wind direction (WD), relative humidity (RH), air pressure, temperature, and
121 precipitation were measured by an automatic weather monitoring system. The planetary boundary height was
122 obtained from the European Centre for Medium-Range Weather Forecasts
123 ([https://www.ecmwf.int/en/forecasts/datasets/browse-reanalysis -datasets](https://www.ecmwf.int/en/forecasts/datasets/browse-reanalysis-datasets)).

124 **2.2 Ozone formation potential (OFP) and secondary formation potential (SOAFP) calculation**
125 The formation potential of O₃ and SOA was used to characterize the relative importance of VOCs species and
126 sources in secondary formation, which were estimated using Eqs. (1) and (2).

$$127 OFP = \sum_i^n MIR_i \times [VOC(ppb)]_i \quad (1)$$

$$128 SOAFP = \sum_i^n Y_i \times [VOC(ppb)]_i \quad (2)$$

129 where n represents the number of VOCs, [VOC] $_i$ represents the i th VOC species concentration, MIR $_i$ is the
130 maximum incremental reactivity for the i th VOC species, and Y_i is the SOA yield of VOC $_i$ (McDonald et al.,
131 2018). The MIR for each VOC species were taken from the updated Carter research results
132 (<http://www.engr.ucr.edu/~carter/reactdat.htm>, last access: 24 February 2021). For species lacking yield curves,
133 the fractional aerosol coefficient (FAC) values proposed by Grosjean and Seinfeld (1989) were used.

134 **2.3 Deweathered model**

135 In this work, the influences of meteorological conditions on O_3 and $PM_{2.5}$ were removed using the random forest
136 (RF) model. The meteorological predictors in the RF model include wind speed (WS), wind direction (WD), air
137 temperature (T), relative humidity (RH), precipitation (Prec), air pressure (P), time predictors (year, day of year
138 (DOY), hour) and planetary boundary layer height (BLH). These meteorological parameters have been reported
139 to be strongly associated with $PM_{2.5}$ and O_3 concentrations in various regions in China (Chen et al., 2020; Feng
140 et al., 2020) and contributed significantly in previous $PM_{2.5}$ and O_3 prediction models (She et al., 2020; Li et al.,
141 2020). The modelling relates the hourly variability of O_3 and $PM_{2.5}$ to that of meteorological variables. The model
142 performance was evaluated through 10-fold cross validation (CV) approach, which The original dataset was
143 randomly selects 10% of the dataset for model testing and trains the model with the remaining data. eclassified
144 into a training dataset (90 % of input dataset) for developing the RF model, and the remaining one was treated as
145 the test dataset. This process was repeated ten times, and each record was selected once as testing data. In each
146 round, the training dataset includes ~90% randomly selected data representing different seasons. After the
147 building of the RF model, the deweathered technique was applied to predict the air pollutant level at a specific
148 time point. The differences in original pollutant concentrations and deweathered pollutant concentrations were
149 regarded as the concentrations contributed by meteorology. Statistical indicators including R^2 , RMSE, and MAE
150 values were regarded as the major criteria to evaluate the modeling performance.

151 **2.4 Positive matrix factorization (PMF)**

152 In this study, the US EPA PMF 5.0 software was used for VOCs source apportionment (Abeleira et al., 2017; Li
153 et al., 2019a; Xue et al., 2017). The detailed description of the PMF model is found elsewhere (Ling et al., 2011;
154 Yuan et al., 2009). PMF uses both concentration and user-provided uncertainty associated with the data to weight
155 individual points. Species with high percentages of missing values ($> 40\%$) and with signal-to-noise ratio of

156 below 2 were excluded. Based on this, 53 VOC species including source tracers (e.g., chloromethane,
157 trichloroethylene, tetrachloroethylene and MTBE) and SO₂ were chosen for the source apportionment analysis.
158 Data values below the MDL were replaced by MDL/2, and the missing data were substituted with median
159 concentrations. If the concentration is less than or equal to the MDL provided, the uncertainty is calculated using
160 the equation of Unc = 5/6 × MDL; if the concentration is greater than the MDL provided, the uncertainty is
161 calculated as Unc = [(error fraction × mixing ratio)² + (MDL)²]^{1/2}.

162 During the PMF analysis, the bootstraps (BS) method, displacement (DISP) analysis, and the combination
163 of the DISP and BS (BS–DISP) were used to evaluate the uncertainty of the base run solution. A total of 100
164 bootstrap runs were performed, and acceptable results were gained for all factors (above 90%). Based on the
165 DISP analysis, the observed drop in the *Q* value was below 0.1 %, and no factor swap occurred, confirming that
166 the solution was stable. The BS–DISP analysis showed that the observed drop in the *Q* value was less than 0.5 %,
167 demonstrating that the solution was useful.

168 **3. Results and discussion**

169 **3.1 TVOC mixing ratios and chemical composition**

170 The time series of meteorological parameters and concentrations of air pollutants during the measurement period
171 are shown in Fig. 1. The ambient temperature ranged from -13.3°C to 38.7°C and the RH varied between 5% and
172 99% across the sampling months. Prevailing winds shifted between southwesterly and northeasterly with WS of
173 0–6.8 m s⁻¹. The mixing ratio of total VOCs (TVOC) ranged from 5.5–118.7 ppbv during the sampling period
174 with relatively higher values during September and November (49.9-51.6 ppbv) while relatively lower values
175 (22.2-27.5 ppbv) across the other months. Major VOC compositions were generally consistent during the whole
176 measurement period. Alkanes, OVOCs and halocarbons were the dominant chemical groups, accounting for 75–

177 81% of the TVOCs across the sampling months. In terms of individual species, acetone, dichloromethane, n-
178 butane, toluene, methyl tert butyl ether (MTBE), isot-pentane, propylene, n-hexane, 1,1-dichloroethane, benzene
179 and 1-butene made up the largest contribution, accounting for 50.6 % of the TVOC on average during the whole
180 measurement period.

181 As shown in Fig. 2, The comparison of concentration and composition of chemical groups observed in this
182 work and previous studies is shown in Fig. 2. Clearly, the concentrations of TVOCs and major VOC groups
183 including alkanes, alkenes, aromatics, halocarbons and OVOCs observed in this study were apparently lower
184 than those during the sampling months in 2014 and 2016 in urban sites in Beijing (An et al., 2012; Liu et al.,
185 2020a; Li et al., 2015b), indicating the effectiveness of control measures in most recent years on lowering VOCs
186 emission. Besides, the composition of major chemical groups also showed remarkable changes, with decreased
187 proportions of alkanes while increased fractions of halocarbons, aromatics and OVOCs, reflecting the changes
188 in emission sources types in most recent years.

189 During the measurement period, 14 O₃ pollution episodesdays (days with maximum 8-h average O₃
190 exceeding 160 $\mu\text{g m}^{-3}$) were observed, (i.e., on 17-22 April, 3-17 May, 16 May, 18-29 June, 24-25 June,
191 2-13 July, 5 July, 13 July, 25-26 September and 25-29 September of 2019), respectively. and April, May,
192 June, July, and September of 2019 were defined as the O₃-polluted months. The comparison of meteorological
193 parameters and air pollutanttrace gases on O₃ pollution and compliance days (days with maximum 8-h average
194 O₃ below 160 $\mu\text{g m}^{-3}$) eduringf the fourfive O₃-polluted months (i.e., April, May, June, July, and September of
195 2019) is discussed hereshown in Fig. 3. As shown in Fig. 3, the WS on O₃ pollution days ($1.31 \pm 0.90 \text{ m s}^{-1}$)
196 was slightly lower than that on O₃ compliance days ($1.47 \pm 1.10 \text{ m s}^{-1}$), indicating that precursors were more
197 conductive to be diluted on O₃ compliance days. The variation trend of O₃ and temperature displayed the negative

198 correlation, and the linear correlations between O₃ and temperature on O₃ pollution days ($R^2 = 0.63$) was stronger
199 than that on O₃ compliance days ($R^2 = 0.35$). The mean TVOC concentration on O₃ pollution days (32.3 ppbv)
200 was higher than that on O₃ compliance days (29.6 ppbv), which was mainly attributed to higher concentrations
201 of MTBE, acrolein, trans-2-butene on pollution days. MTBE is widely used as a fuel additive in motor gasoline
202 (Liang et al., 2020), and trans-2-butene is the main component of oil/gas evaporation (Li et al., 2019a). Such
203 result suggested enhanced contribution of traffic emissions on O₃ pollution days. Besides, the concentration of
204 isoprene, which is primarily produced by vegetation through photosynthesis, increased significantly on O₃
205 pollution days probably due to the stronger plant emission at elevated temperature (Guenther et al., 1993, 2012;
206 Stavrakou et al., 2014). The ratio of *m/p*-xylene to ethylbenzene (X/E) measured can be used as an indicator of
207 the photochemical aging of air masses because of their similar sources in urban environments and differences in
208 atmospheric lifetimes (Carter., 2010; Miller et al., 2012; Wang et al., 2013a). The mean X/E value on O₃
209 compliance days (1.41) was higher than that on O₃ pollution days (1.17), indicating enhanced secondary
210 transformation of VOCs on O₃ pollution days.

211 The daily PM_{2.5} concentrations ranged from 9-260 $\mu\text{g m}^{-3}$ with the mean value of 88.5 $\mu\text{g m}^{-3}$ during the
212 measurement period. 15 PM_{2.5} pollution days (daily average PM_{2.5} exceeding 75 $\mu\text{g m}^{-3}$) were observed(i.e., on
213 ~~1-2 December and 5 December of 2018,~~ 3 January, 12-13 January, 22-23 April, 29 April, 12 May, 15 May, 19
214 October, ~~and~~ 21-23 November of 2019, 1-2 December and 5 December of 2018), ~~respectively. and December~~
215 ~~of 2018, January, April, May, October and November of 2019 were identified as the PM_{2.5} polluted months.~~
216 During the six PM_{2.5}-polluted months (i.e., December of 2018, January, April, May, October and November of
217 2019), the WS on PM_{2.5} pollution days ($1.05 \pm 1.06 \text{ m s}^{-1}$) was lower than that on PM_{2.5} compliance days (1.43
218 $\pm 1.06 \text{ m s}^{-1}$), indicating the weaker ability of winds for the dilution and diffusion of precursor on PM_{2.5} pollution

219 days. ~~Both the value of relative humidity (RH) and TVOCs increased significantly on PM_{2.5} pollution days,~~
220 ~~suggesting that the secondary transformation of VOCs was more conducive at higher RH.~~ The mean X/E value
221 on PM_{2.5} compliance days (1.47) was slightly higher than that on PM_{2.5} pollution days (1.44), indicating enhanced
222 secondary transformation of VOCs on PM_{2.5} pollution days.

223 **3.2 The role of VOCs on secondary pollution**

224 **3.2.1 Estimating O₃ and PM_{2.5} levels contributed by emissions**

225 O₃ and secondary aerosols are primarily formed via photochemical reactions in the atmosphere, of which
226 concentrations could be largely influenced by meteorological conditions (Chen et al., 2020; Feng et al., 2020;
227 Zhai et al., 2019). In this work, the respective contributions of meteorology and emissions to PM_{2.5} and O₃
228 variations were determined using the RF model as described in section 2.3. The coefficients of determination (R^2)
229 for the RF model in predicting PM_{2.5} and O₃ are 0.85 and 0.91, respectively (Shown in Fig. S2). The respective
230 contributions of anthropogenic and meteorology to O₃ and PM_{2.5} during each period is shown in Fig. 4. During
231 the O₃-polluted months, the meteorologically-driven O₃ level on O₃ pollution days (72.5 $\mu\text{g m}^{-3}$) was significantly
232 higher than that on O₃ compliance days (35.3 $\mu\text{g m}^{-3}$). After removing the meteorological contribution, the
233 residual emission-driven O₃ level on O₃ pollution (45.3 $\mu\text{g m}^{-3}$) and compliance days (44.9 $\mu\text{g m}^{-3}$) of the O₃-
234 polluted months was almost identical and were significantly higher than that during the non-O₃-polluted months
235 (23.8 $\mu\text{g m}^{-3}$). The emission-driven PM_{2.5} level was in the order of: PM_{2.5} pollution days of the PM_{2.5}-polluted
236 months (55 $\mu\text{g m}^{-3}$) > PM_{2.5} compliance days of the PM_{2.5}-polluted months (44 $\mu\text{g m}^{-3}$) > non-PM_{2.5}-polluted
237 months (29 $\mu\text{g m}^{-3}$). These results suggested that apart from meteorological factors, emissions also play a role in
238 deteriorating PM_{2.5} and O₃ pollution, and reducing anthropogenic emissions is essential for improving air quality.

239 The VOCs/NO_x ratio has been widely used to distinguish whether the O₃ formation is VOC limited or NO_x
240 limited (Li et al., 2019a). Generally, VOC-sensitive regime occurs when VOCs/NO_x ratios are below 10 while
241 NO_x-sensitive regime occurs when VOCs/NO_x ratios are higher than 20 (Hanna et al., 1996; Sillman, 1999). In
242 this study, the values of VOCs/NO_x (ppbv ppbv⁻¹) were all below 3 during both the O₃-polluted and non-O₃-
243 polluted months (Fig. S3), suggesting that the O₃ formation was sensitive to VOCs, and thus the reductions of
244 the emissions of VOCs will be beneficial for O₃ alleviation.

245 **3.2.2 Contribution of VOCs to OFP and SOAfp**

246 As discussed in 3.1, O₃ formation was generally VOCs-sensitive during the measurement period. Quantifying the
247 contribution of speciated VOCs species to O₃ is helpful for developing effective VOCs control measures and
248 alleviating O₃ pollution. The averaged OFP on O₃ pollution days of the O₃-polluted months, O₃ compliance days
249 of the O₃-polluted months, and during the non-O₃-polluted months were 224.9, 201.4, and 187.5 $\mu\text{g m}^{-3}$,
250 respectively (Fig. 5). According to our observations, the higher OFP on O₃ pollution days than that on O₃
251 compliance days during the O₃-polluted months was mainly attributed to higher levels of trans-2-butene, o-xylene
252 and acrolein O₃ on pollution days, in line with that in Fig. 3. Alkenes, aromatics and OVOCs were the three
253 biggest contributors to O₃ formation, accounting for 85.1%, 85.7% and 81.6% of the total OFP on O₃ pollution
254 days of the O₃-polluted months, O₃ compliance days of the O₃-polluted months, and during the non-O₃-polluted
255 months, respectively. In terms of the individual species, the top 10 highest contributors during the O₃-polluted
256 months were toluene (~~7.5% and 6.4%~~ and 7.5% on O₃ compliance and polluted pollution and compliance days,
257 respectively), trans-2-butene (~~7.5% and 9.6%~~ and 7.5%), acrolein (~~5.7% and 10.8%~~ and 5.7%), m/p-xylene (~~6.9%~~
258 and 6.1% and 6.9%), o-xylene (~~5.8% and 6.6%~~ and 5.8%), 1-butene (~~7.1% and 5.2%~~ and 7.1%), 1-hexene (~~5.4%~~
259 and 4.4% and 5.4%), vinyl acetate (~~5.7% and 4.2%~~ and 5.7%), methyl methacrylate (~~4.8% and 5.5%~~ and 4.8%),

260 and 1-pentene (~~4.4%~~ and 4.5% and 4.4%). During the non-O₃-polluted months, the overall OFP was mainly
261 contributed by toluene (10.8%), trans-2-butene (10.5%), 1-butene (7.3%), m/p-xylene (6.5%), 1-pentene (5.7%),
262 1-hexene (5.0%), methyl methacrylate (4.9%), o-xylene (4.9%), vinyl acetate (3.8%), and isopentane (2.3%),
263 respectively.

264 As shown in Fig. S3, the ratio of VOCs/NO_x was generally below 3 during the sampling period, indicating
265 high NO_x conditions. Based on the estimated yields of the VOCs shown in Table S2, the SOAFPs were calculated
266 and compared in Fig. 5. The mean SOAFP on PM_{2.5} pollution days of the PM_{2.5}-polluted months, PM_{2.5}
267 compliance days of the PM_{2.5}-polluted months, and during the non-PM_{2.5}-polluted months were 1.28, 1.07, and
268 0.89 $\mu\text{g m}^{-3}$. During the six PM_{2.5}-polluted months, the higher SOAFP on PM_{2.5} pollution days than that on PM_{2.5}
269 compliance days was mainly attributed to higher levels of 1,2,4-trimethylbenzene, n-~~undecane~~undecanone, n-
270 ~~nonane~~Nonane, 1,4-diethylbenzene, and 1,3-diethylbenzene on PM_{2.5} pollution days. Aromatics have the largest
271 SOAFP, accounting for 74% and 75% of the total SOAFP on PM_{2.5} pollution and compliance days of the PM_{2.5}-
272 polluted months, and 70% of the total SOAFP during the non-PM_{2.5}-polluted months, respectively. The 10 species
273 responsible for most of the SOAFP were toluene (41% and 40% on PM_{2.5} pollution and compliance days of the
274 PM_{2.5}-polluted months, and 33% during the non-PM_{2.5}-polluted months), 1-hexene (13.0%, 12.5%, and 15.2%),
275 xylenes (11.6%, 14.1% and 14.8%), ethylbenzene (4.9%, 5.3% and 6.0%), styrene (4.5%, 5.6% and 5.6%), 1-
276 pentene (3.3%, 3.4% and 4.3%), methyl cyclopentane (2.1%, 2.7% and 3.6%), 1,2,3-trimethylbenzene (2.8%,
277 2.4% and 2.8%), m-ethyl toluene (1.7%, 1.4% and 1.7%) and p-ethyl toluene (1.7%, 1.4% and 1.7%), respectively.

278 **3.3 Source apportionment of VOCs**

279 **3.3.1 Indication from tracers**

280 The great changes in the mixing ratios of ~~VOCs different~~ species are mainly affected by the photochemical

281 processing and the emission inputs, and ~~ambient~~ ratios ~~for of~~ VOCs species having similar atmospheric lifetimes
282 ~~can reflect the source features are indicators of different sources~~ (Li et al., 2019a; Raysoni et al., 2017 Song et al.,
283 2021). The ratio of *i*-pentane to *n*-pentane are widely used to examine the impact of vehicle emissions, fuel
284 evaporation and combustion emissions, within the *i/n*-pentane ratios of ranging between 2.2–3.8, 1.8–4.6 and
285 0.56–0.80, respectively (McGaughey et al., 2004; Jobson et al., 2004; Russo et al., 2010; Wang et al., 2013b; Yan
286 et al., 2017). As shown in Fig. 6, the *i/n*-pentane ratios during the PM_{2.5}-polluted months were mostly within the
287 range of 0.3–2.0, suggesting the pentanes were from the mixed sources of coal combustion and fuel evaporation.
288 During the non-PM_{2.5}-polluted months, the *i/n*-pentane ratios were distributed in the range of 1.3–3.4, indicating
289 strong impacts from vehicle exhaust and fuel evaporation. During the O₃-polluted months, most of the *i/n*-
290 pentane ratios (1.5–2.5) were distributed within the reference range of vehicle exhaust and fuel evaporation,
291 whereas most of the *i/n*-pentane ratios during the non-O₃-polluted months ranged between 1.7–2.1, suggesting
292 the significant impact of fuel evaporation.

293 The toluene/benzene (T/B) ratio, a widely used indicator for sources of aromatics. In areas heavily impacted
294 by vehicle emissions, the T/B ratio lies in the range of 0.9–2.2 (Qiao et al., 2012; Dai et al., 2013; Wang et al.,
295 2013c; Yao et al., 2013; Zhang et al., 2013; Yao et al., 2015a; Mo et al., 2016; Deng et al., 2018). Higher T/B
296 ratios were reported for solvent use (greater than 8.8) (Yuan et al., 2010; Wang et al., 2014b; Zheng et al., 2013)
297 and industrial processes (1.4–5.8) (Mo et al., 2015; Shi et al., 2015). In burning source emission studies, the T/B
298 ratio was below 0.6 in different combustion process and raw materials (Tsai et al., 2003; Akagi et al., 2011; Mo
299 et al., 2016). Most of the T/B ratios during the PM_{2.5}-polluted and non-PM_{2.5}-polluted months were within the
300 range of 1.1–1.8 and 0.8–2.2, whereas the T/B ratios were mostly distributed within the range of 0.8–2.2 and 0.9–
301 1.9 during the O₃-polluted and non-O₃-polluted months, respectively, suggesting the significant impact of vehicle

302 and industrial emissions.

303 **3.3.2 PMF**

304 The factor profiles given by PMF and the contribution of each source to ambient VOCs during each period is
305 presented in Fig. 7 and Fig. 8, respectively. Six emission sources were identified: coal/biomass burning, solvent
306 use, industrial sources, oil gas evaporation, gasoline vehicle emission, and diesel vehicle emission based on the
307 corresponding markers for each source category. In general, diesel vehicle exhaust, gasoline vehicle exhaust and
308 industrial emissions were the main VOCs sources during both the O₃-polluted and PM_{2.5}-polluted months, with
309 total contributions of 62% and 62% on O₃ pollution and compliance days of the O₃-polluted months, and 66%
310 and 59% on PM_{2.5} pollution and compliance days of the PM_{2.5}-polluted months, respectively. The O₃-polluted
311 months exhibited higher proportions of diesel (24% on O₃ compliance days and 27% on O₃ pollution days) and
312 gasoline vehicle emission (17% on O₃ compliance days and 16% on O₃ pollution days) compared with the non-
313 O₃-polluted months (8% and 13%, respectively). During the O₃-polluted months, the contributions of industrial
314 emissions (22%) and fuel evaporation (18%) on O₃ pollution days were much higher than those on O₃ compliance
315 days (18% and 13%, respectively). Figure 9 presents the relative contributions of individual VOC sources from
316 PMF to OFP. On the base of O₃ formation impact, diesel and gasoline vehicle exhaust were major contributors.
317 During the O₃-polluted months, vehicle emissions and fuel evaporation showed higher OFP values on O₃
318 pollution days (93.9 and 35.5 $\mu\text{g m}^{-3}$) compared with those on O₃ compliance days (88.0 and 25.8 $\mu\text{g m}^{-3}$,
319 respectively). Although industrial emissions act as an important source for VOCs concentrations on O₃-pollution
320 days (shown in Fig. 8), the potential to form O₃ is limited, accounting for 11% of the total OFP. As illustrated in
321 Fig. 7, the industrial source was distinguished by high compositions of alkanes while relatively lower

322 compositions of alkenes and aromatics, resulting in low O₃ formation potentials. Such results suggested that the
323 fuel use and diesel vehicle exhaust should be controlled preferentially for O₃ mitigation.

324 The PM_{2.5}-polluted months showed higher proportions of industrial (29% on both PM_{2.5} compliance and
325 PM_{2.5} pollution days) and coal/biomass combustion emissions (16% on PM_{2.5} compliance days and 18% on PM_{2.5}
326 pollution days) compared with the non-PM_{2.5}-polluted months (17% and 10%, respectively). The PM_{2.5} pollution
327 days were dominated by industrial emission (29%), diesel vehicle exhaust (24%), and combustion source (18%).
328 During the PM_{2.5}-polluted months, the contribution of diesel vehicle exhaust on PM_{2.5} pollution days (24%) was
329 higher than that on PM_{2.5} compliance days (16%). On the base of PM_{2.5} formation impact, diesel vehicle exhaust
330 and combustion were two major contributors on PM_{2.5} pollution days (shown in Fig. 9), and these two sources
331 showed obvious higher SOA FP on PM_{2.5} pollution days (0.30 and 0.32 $\mu\text{g m}^{-3}$, respectively) compared with those
332 on PM_{2.5} compliance days of the PM_{2.5}-polluted months (0.15 and 0.14 $\mu\text{g m}^{-3}$, respectively). Although industrial
333 emissions act as an important source for VOCs concentrations on PM_{2.5} pollution days, the potential to form PM_{2.5}
334 is limited, accounting for 16% of the total SOA FP. The above results suggested that diesel vehicle exhaust and
335 combustion should be controlled preferentially for alleviating PM_{2.5} pollution.

336 Based on the mass concentrations of individual species in each source, m/p-xylene, o-xylene, methyl
337 methacrylate, vinyl acetate, 1-hexene, and acrolein in gasoline and diesel vehicular emissions; toluene, trans-2-
338 butene, and 1-pentene in fuel evaporation and diesel vehicular emissions; acrolein in solvent, gasoline vehicular
339 and diesel vehicular emissions were the dominant species contributing to photochemical O₃ formation (Fig. 10).
340 Toluene, m/p-xylene, o-xylene, styrene, ethylbenzene, 1-pentene, 1,2,3-trimethylbenzene from combustion and
341 diesel vehicular emissions; 1-hexene from diesel vehicular emission; and methyl cyclopentane from combustion,

342 industrial and diesel vehicular emissions were the dominant contributors for SOA formation during the PM_{2.5}
343 pollution periods (Fig. 10).

344 **3.4 Limitation**

345 This study analyzed the VOC sources and their contributions to O₃ and SOA formation across different seasons.
346 It should be pointed out that the sampling campaign for VOCs measurement was not conducted continuously
347 during December 2018 and November 2019. For instance, the air samples were not collected in August and
348 February-March of 2019, during which the pollution events of O₃ and PM_{2.5} occurred, respectively. The variations,
349 sources and secondary transformation potentials of VOCs, particularly for O₃ and PM_{2.5} pollution periods cannot
350 be fully depicted. Despite the uncertainties that remained, the results obtained in this study provide useful
351 information for VOCs emission control strategy and assist overcoming air pollution issue in Beijing.

352 **4. Conclusions**

353 In this work, the field sampling campaign of VOCs was conducted at urban Beijing ~~during from~~ December 2018
354 ~~and to~~ November 2019. The VOCs concentrations ranged from 5.5 to 118.7 ppbv with mean value of 34.9 ppbv.

355 Alkanes, OVOCs and halocarbons were the dominant chemical groups, accounting for 75-81% of the TVOCs
356 across the sampling months. By excluding the meteorological impact, the emission-driven O₃ level during the
357 O₃-polluted months were higher than that during the non-O₃-polluted months, and similar pattern was found for
358 PM_{2.5}. The molar ratio of VOCs to NO_x indicated that O₃ formation was limited by VOCs during both the O₃-
359 polluted non-O₃-polluted months, and thus reducing VOCs emission is essential for alleviation of O₃ pollution.

360 The contributions of coal/biomass combustion, solvent use, industrial sources, oil/gas evaporation, gasoline
361 exhaust, and diesel exhaust were identified based on PMF analysis. Considering both the concentration and
362 maximum incremental reactivity of individual VOC species for each source, fuel use and diesel exhaust sources

363 were identified as the main contributors of O₃ formation during the O₃-polluted months, particularly the VOCs
364 species of toluene, xylenes, trans-2-butene, acrolein, methyl methacrylate, vinyl acetate, 1-butene and 1-hexene,
365 illustrating the necessity of conducting emission controls on these pollution sources and species for alleviating
366 O₃ pollution. VOCs from diesel vehicles and combustion were found to be the dominant contributors for SOAFP,
367 particularly the VOC species of toluene, 1-hexene, xylenes, ethylbenzene and styrene, and top priority should be
368 given to these for the alleviation of haze pollution.

369 **Acknowledgements**

370 ~~This work was supported by the National Natural Science Foundation of China (92044302) and the Beijing~~
371 ~~Municipal Science and Technology Project (Z211100004321006 & Z191100009119001).~~

372 **Data availability**

373 The meteorological data are available at <http://data.cma.cn/> (China Meteorological Administration). The website
374 can be browsed in English <http://data.cma.cn/en>. The concentrations of air pollutants including PM_{2.5}, O₃ and
375 NO_x are available at <https://air.cnemc.cn:18007/> (Ministry of Ecology and Environment the People's Republic of
376 China). The website can be browsed in English <http://english.mee.gov.cn/>. The daily mixing ratio of individual
377 VOCs species is given in Table S1 in the Supplement.

378 **Author Contributions**

379 DW designed the study and performed the VOCs measurement. QX and RH assists in air sampling and data
380 collection. LC performed the data analysis and wrote the paper with contributions from all co-authors. SW and
381 JH reviewed the paper and provided comments for improving the paper.

382 **Competing interests**

383 The authors declare that they have no conflict of interest.

384 **Acknowledgements**

385 This work was supported by the National Natural Science Foundation of China (92044302) and the Beijing

386 Municipal Science and Technology Project (Z211100004321006 & Z191100009119001).

387 **References**

388 Abeleira, A., Pollack, I. B., Sive, B., Zhou, Y., Fischer, E. V., Farmer, D. K., 2017. Source characterization of
389 volatile organic compounds in the Colorado Northern Front Range Metropolitan Area during spring and summer
390 2015, *J. Geophys. Res.-Atmos.*, 122, 3595–3613, <https://doi.org/10.1002/2016jd026227>.

391 Ahmad, W., Coeur, C., Tomas, A., Fagniez, T., Brubach, J. B., Cuisset, A., 2017. Infrared spectroscopy of
392 secondary organic aerosol precursors and investigation of the hygroscopicity of SOA formed from the OH
393 reaction with guaiacol and syringol. *Appl. Opt.* 56, E116, <https://doi.org/10.1364/AO.56.00E116>.Akagi, S. K.,
394 Yokelson, R. J., Wiedinmyer, C., Alvarado, M. J., Reid, J. S., Karl, T., Crounse, J. D., Wennberg, P. O., 2011.
395 Emission factors for open and domestic biomass burning for use in atmospheric models. *Atmos. Chem. Phys.* 11,
396 4039–4072.

397 Atkinson, R., 2000. Atmospheric chemistry of VOCs and NO_x. *Atmos. Environ.* 34, 2063–2101.

398 An, J.L., Wang, Y.S., Wu, F.K., Zhu, B., 2012. Characterizations of volatile organic compounds during high
399 ozone episodes in Beijing, China. *Environ. Monit. Assess.* 184, 1879e1889.

400 Carter, W.P.L. and Atkinson, R., 1989. Computer modeling study of incremental hydrocarbon reactivity. *Environ.*
401 *Sci. Technol.* 23, 864–880, <https://doi.org/10.1021/es00065a017>.

402 Carter, W.P.L., 2010. Development of the SAPRC-07 chemical mechanism, *Atmos. Environ.* 44, 5324–5335,
403 <https://doi.org/10.1016/j.atmosenv.2010.01.026>.

404 Chang, T.Y. and Rudy, S.J., 1990. Ozone-forming potential of organic emissions from alternative-fueled vehicles,
405 *Atmos. Environ.*, 24, 2421–2430, [https://doi.org/10.1016/0960-1686\(90\)90335-K](https://doi.org/10.1016/0960-1686(90)90335-K).

406 Chen, L., Zhu, J., Liao, H., Yang, Y., Yue, X., 2020. Meteorological influences on PM_{2.5} and O₃ trends and
407 associated health burden since China's clean air actions, *Sci. Total Environ.* 744, 140837,
408 <https://doi.org/10.1016/j.scitotenv.2020.140837>.

409 Dai, P., Ge, Y., Lin, Y., Su, S., and Liang, B., 2013. Investigation on characteristics of exhaust and evaporative
410 emissions from passenger cars fueled with gasoline/methanol blends. *Fuel.* 113, 10–16.

411 Deng, C. X., Jin, Y. J., Zhang, M., Liu, X. W., Yu, Z.M., 2018. Emission Characteristics of VOCs from On-Road
412 Vehicles in an Urban Tunnel in Eastern China and Predictions for 2017–2026. *Aerosol Air Qual. Res.* 18, 3025–
413 3034.

414 Doumbia, T., Granier, C., Elguindi, N., Bouarar, I., Darras, S., Brasseur, G., Gaubert, B., Liu, Y., Shi, X.,
415 Stavrakou, T., Tilmes, S., Lacey, F., Deroubaix, A., Wang, T., 2021. Changes in global air pollutant emissions
416 during the COVID-19 pandemic: a dataset for atmospheric modeling. *Earth Syst. Sci. Data.* 13, 4191–4206.

417 Fan, H., Zhao, C., Yang, Y., 2020. A Comprehensive Analysis of the Spatio-Temporal Variation of Urban Air
418 Pollution in China During 2014–2018, *Atmos. Environ.*, 220, 117066,
419 <https://doi.org/10.1016/j.atmosenv.2019.117066>.

420 Feng, J., Liao, H., Li, Y., Zhang, Z., Tang, Y., 2020. Long-term trends and variations in haze-related weather
421 conditions in north China during 1980–2018 based on emission-weighted stagnation intensity. *Atmos. Environ.*
422 240, 117830, <https://doi.org/10.1016/j.atmosenv.2020.117830>.

423 Fu, Y., Liao, H., Yang, Y., 2019. Interannual and Decadal Changes in Tropospheric Ozone in China and the
424 Associated Chemistry Climate Interactions: A Review, *Adv. Atmos. Sci.* 36, 975–993.

425 Gani, S., Bhandari, S., Seraj, S., Wang, D. S., Patel, K., Soni, P., Arub, Z., Habib, G., Hildebrandt Ruiz, L., Apte,
426 J. S., 2019. Submicron aerosol composition in the world's most polluted megacity: the Delhi Aerosol Supersite
427 study. *Atmos. Chem. Phys.* 19, 6843–6859.

428 Grosjean, D., and Seinfeld, J. H., 1989. Parameterization of the formation potential of secondary organic aerosols,
429 *Atmos. Environ.*, 23, 1733-1747, 10.1016/0004- 6981(89)90058-9.

430 Guenther, A.B., Zimmerman, P.R., Harley, P.C., Monson, R.K., Fall, R., 1993. Isoprene and monoterpene
431 emission rate variability: Model evaluations and sensitivity analyses. *J. Geophys. Res. Atmos.* 98, 12609–12617,
432 <https://doi.org/10.1029/93JD00527>.

433 Han, S., Zhao, Q., Zhang, R., Liu, Y., Li, C., Zhang, Y., Li, Y., Yin, S., Yan, Q., 2020. Emission characteristic
434 and environmental impact of process-based VOCs from prebaked anode manufacturing industry in Zhengzhou,
435 China. *Atmos. Pollut. Res.* 627 11, 67-77, 10.1016/j.apr.2019.09.016.

436 Hanna, S. R., Moore, G. E., Fernau, M., 1996. Evaluation of photochemical grid models (UAM-IV, UAM-V,
437 and the ROM/UAMIV couple) using data from the Lake Michigan Ozone Study (LMOS). *Atmos. Environ.* 30,
438 3265–3279.

439 Hong, Z., Li, M., Wang, H., Xu, L., Hong, Y., Chen, J., Chen, J., Zhang, H., Zhang, Y., Wu, X., Hu, B., Li, M.,
440 2019. Characteristics of atmospheric volatile organic compounds (VOCs) at a mountainous forest site and two
441 urban sites in the southeast of China. *Sci. Total. Environ.* 657, 1491–1500,
442 <https://doi.org/10.1016/j.scitotenv.2018.12.132>.

443 Huang, R.J., Zhang, Y., Bozzetti, C., Ho, K.F., Cao, J.J., Han, Y., Daellenbach, K. R., Slowik, J. G., Platt, S. M.,
444 Canonaco, F., Zotter, P., Wolf, R., Pieber, S. M., Bruns, E. A., Crippa, M., Ciarelli, G., Piazzalunga, A.,
445 Schwikowski, M., Abbaszade, G., Schnelle-Kreis, J., Zimmermann, R., An, Z., Szidat, S., Baltensperger, U., El

446 Haddad, I., Prevot, A.S.H., 2014. High secondary aerosol contribution to particulate pollution during haze events
447 in China, *Nature*, 514, 218-222, 10.1038/nature13774.

448 Jobson, B. T., Berkowitz, C. M., Kuster, W. C., Goldan, P. D., Williams, E. J., Fesenfeld, F. C., Apel, E. C., Karl,
449 T., Lonneman, W. A., Riemer, D., 2004. Hydrocarbon source signatures in Houston, Texas: Influence of the
450 petrochemical industry. *J. Geophys. Res. Atmos.* 109, D24305, <https://doi.org/10.1029/2004jd004887>.

451 Kuang, Y., He, Y., Xu, W.Y., Yuan, B., Zhang, G., Ma, Z.Q., Wu, C.H., Wang, C.M., Wang, S.H., Zhang, H.Y.,
452 Tao, J.C., Ma, N., Su, H., Cheng, Y.F., Shao, M., Sun, Y.L., 2020. *Environ Sci & Techno.* 54 (7), 3849-3860.

453 Li, L., Chen, Y., Zeng, L., Shao, M., Xie, S., Chen, W., Lu, S., Wu, Y., Cao, W., 2014. Biomass burning
454 contribution to ambient volatile organic compounds (VOCs) in the Chengdu–Chongqing Region (CCR), China.
455 *Atmos. Environ.* 99, 403–410.

456 Li, J., Xie, S.D., Zeng, L.M., Li, L.Y., Li, Y.Q., Wu, R.R., 2015. Characterization of ambient volatile organic
457 compounds and their sources in Beijing, before, during, and after Asia-Pacific Economic Cooperation China
458 2014. *Atmos. Chem. Phys.* 15, 7945–7959

459 Li, G., Bei, N., Cao, J., Wu, J., Long, X., Feng, T., Dai, W., Liu, S., Zhang, Q., Tie, X., 2017a. Widespread and
460 persistent ozone pollution in eastern China during the non-winter season of 2015: observations and source
461 attributions, *Atmos. Chem. Phys.*, 17, 2759–2774, <https://doi.org/10.5194/acp-17-2759-2017>.

462 Li, Y. J., Sun, Y., Zhang, Q., Li, X., Li, M., Zhou, Z., Chan, C. K., 2017b. Real-time chemical characterization
463 of atmospheric particulate matter in China: A review, *Atmos. Environ.*, 158, 270–304.

464 Li, B., Ho, S.S.H., Gong, S., Ni, J., Li, H., Han, L., Yang, Y., Qi, Y., Zhao, D., 2019a. Characterization of VOCs
465 and their related atmospheric processes in a central Chinese city during severe ozone pollution periods. *Atmos.*
466 *Chem & Phys.* 19, 617-638.

467 Li, K., Jacob, D.J., Liao, H., Shen, L., Zhang, Q., Bates, K.H., 2019c. Anthropogenic Drivers of 2013–2017
468 Trends in Summer Surface Ozone in China. *Proc. Natl. Acad. Sci.* 116, 422–427.

469 Li, K., Li, J., Tong, S., Wang, W., Huang, R.-J., Ge, M., 2019d. Characteristics of wintertime VOCs in suburban
470 and urban Beijing: concentrations, emission ratios, and festival effects. *Atmos. Chem & Phys.* 19, 8021-8036.

471 Li, K., Jacob, D.J., Shen, L., Lu, X., De Smedt, I., Liao, H., 2020. Increases in surface ozone pollution in China
472 from 2013 to 2019: anthropogenic and meteorological influences. *Atmos. Chem & Phys.* 20, 11423-11433.

473 Liang, Y., Liu, X., Wu, F., Guo, Y., Xiao, H., 2020. The year-round variations of VOC mixing ratios and their
474 sources in Kuytun City (northwestern China), near oilfields. *Atmos. Pollut. Res.* 11,9
475 DOI:10.1016/j.apr.2020.05.022.

476 Liu, B., Liang, D., Yang, J., Dai, Q., Bi, X., Feng, Y., Yuan, J., Xiao, Z., Zhang, Y., Xu, H., 2016a.
477 Characterization and source apportionment of volatile organic compounds based on 1-year of observational data
478 in Tianjin, China. *Environ. Pollut.* 218, 757–769, <https://doi.org/10.1016/j.envpol.2016.07.072>.

479 Liu, B. S., Liang, D. N., Yang, J. M., Dai, Q. L., Bi, X. H., Feng, Y. C., Yuan, J., Xiao, Z. M., Zhang, Y. F., and
480 Xu, H., 2019b. Characterization and source apportionment of volatile organic compounds based on 1-year of
481 observational data in Tianjin, China. *Environ. Pollut.* 218, 757–769.

482 Liu, Y., Wang, H., Jing, S., Gao, Y., Peng, Y., Lou, S., Cheng, T., Tao, S., Li, L., Li, Y., 2019. Characteristics
483 and sources of volatile organic compounds (VOCs) in Shanghai during summer: Implications of regional
484 transport. *Atmospheric Environment* 215, 116902.

485 Liu, Y.F., Song, M.D., Liu, X.G., Zhang, Y.P., Hui, L.R., Kong, L.W., Zhang, Y.Y., Zhang, C., Qu, Y., An, J.L.,
486 Ma, D.P., Tan, Q.W., Feng, M., 2020a. Characterization and sources of volatile organic compounds (VOCs) and
487 their related changes during ozone pollution days in 2016 in Beijing, China. *Environ Pollut.* 257, 113599.

488 Liu, Y.M., Wang, T., 2020b. Worsening urban ozone pollution in China from 2013 to 2017—Part 2: The effects
489 of emission changes and implications for multi-pollutant control. *Atmos. Chem. Phys.* 20, 6323–6337.

490 Liu, C., Shi, K., 2021. A review on methodology in O₃-NO_x-VOC sensitivity study. *Environmental pollution*,
491 118249.

492 Lu, X., Zhang, L., Wang, X., Gao, M., Li, K., Zhang, Y., Yue, X., Zhang, Y., 2020. Rapid increases in warm-
493 season surface ozone and resulting health impact in China since 2013. *Environ. Sci & Technol Lett.* 7, 240-247.

494 McDonald, B.C., de Gouw, J.A., Gilman, J.B., Jathar, S.H., Akherati, A., Cappa, C.D., Jimenez, J.L., Lee-Taylor,
495 J., Hayes, P.L., McKeen, S.A., Cui, Y.Y., Kim, S.W., Gentner, D.R., Isaacman-VanWertz, G., Goldstein, Allen
496 H., Harley, R.A., Frost, G.J., Roberts, J. M., Ryerson, T.B., Trainer, M., 2018. Volatile chemical products
497 emerging as largest petrochemical source of urban organic emissions, *Science*, 359, 760,
498 <https://doi.org/10.1126/science.aaq0524>.

499 McGaughey, G. R., Desai, N. R., Allen, D. T., Seila, R.L., Lonneman, W. A., Fraser, M. P., Harley, R. A., Pollack,
500 A. K., Ivy, J. M., Price, J. H., 2004. Analysis of motor vehicle emissions in a Houston tunnel during the TexasAir
501 Quality Study 2000. *Atmos. Environ.* 38, 3363 – 3372.

502 Miller, L., Xu, X., Grgicak-Mannion, A., Brook, J., Wheeler, A., 2012. Multi-season, multiyear concentrations
503 and correlations amongst the BTEX group of VOCs in an urbanized industrial city. *Atmos. Environ.* 61, 305–
504 315.

505 Mo, Z., Shao, M., Lu, S., Qu, H., Zhou, M., Sun, J., Gou, B., 2015. Process-specific emission characteristics of
506 volatile organic compounds (VOCs) from petrochemical facilities in the Yangtze River Delta, China. *Sci. Total
507 Environ.* 533, 422–431.

508 Mo, Z., Shao, M., Lu, S., 2016. Compilation of a source profile database for hydrocarbon and OVOC emissions
509 in China. *Atmos. Environ.* 143, 209–217.

510 Odum, J.R., Jungkamp, T.P.W., Griffifin, R.J., Flagan, R.C., Seinfeld, J.H., 1997. The atmospheric aerosol-
511 forming potential of whole gasoline vapor. *Science*. 276, 96–99.

512 Peng, J., Hu, M., Shang, D., Wu, Z., Du, Z., Tan, T., Wang, Y., Zhang, F., Zhang, R., 2021. Explosive secondary
513 aerosol formation during severe haze in the North China Plain. *Environ Sci & Technol.* 55, 2189-2207.

514 Polissar, A.V., Hopke, P.K., Paatero, P., Kaufmann, Y.J., Hall, D.K., Bodhaine, B.A., Dutton, E.G., Harris, J.M.,
515 1999. The aerosol at Barrow, Alaska: long-term trends and source locations. *Atmos. Environ.* 33, 2441–2458,
516 [https://doi.org/10.1016/S1352-2310\(98\)00423-3](https://doi.org/10.1016/S1352-2310(98)00423-3), 1999.

517 Qiao, Y.Z., Wang, H.L., Huang, C., Chen, C.H., Su, L.Y., Zhou, M., Xu, H., Zhang, G.F., Chen, Y.R., Li, L., Chen,
518 M.H., Huang, H.Y., 2012. Source Profile and Chemical Reactivity of VolatileOrganic Compounds from Vehicle
519 Exhaust. *Huanjing Kexue*. 33,1071–1079.

520 Raysoni, A.U., Stock, T.H., Sarnat, J.A., Chavez, M.C., Sarnat, S.E., Montoya, T., Holguin, F., Li, W.W., 2017.
521 Evaluation of VOC concentrations in indoor and outdoor microenvironments at near-road schools. *Environ.*
522 *Pollut.* 231, 681–693.

523

524 Russo, R. S., Zhou, Y., White, M. L., Mao, H., Talbot, R., Sive, B. C., 2010. Multi-year (2004–2008) record of
525 nonmethane hydrocarbons and halocarbons in New England: seasonal variations and regional sources. *Atmos.*
526 *Chem. Phys.* 10, 4909–4929.

527 Sato, K., Takami, A., Isozaki, T., Hikida, T., Shimono, A., Imamura, T., 2010. Mass spectrometric study of
528 secondary organic aerosol formed from the photo-oxidation of aromatic hydrocarbons. *Atmos. Environ.* 44,
529 1080–1087, <https://doi.org/10.1016/j.atmosenv.2009.12.013>.

530 Shao, M., Zhang, Y., Zeng, L., Tang, X., Zhang, J., Zhong, L., Wang, B., 2009. Ground-level ozone in the Pearl
531 River Delta and the roles of VOC and NO_x in its production. *J. Environ. Manage.* 90, 512–518.

532 She, Q., Choi, M., Belle, J. H., Xiao, Q., Bi, J., Huang, K., Meng, X., Geng, G., Kim, J., He, K., Liu, M., Liu, Y.,
533 2020. Satellite-based estimation of hourly PM_{2.5} levels during heavy winter pollution episodes in the Yangtze
534 River Delta, China. *Chemosphere*. 239, 124678, <https://doi.org/10.1016/j.chemosphere.2019.124678>.

535 Shen, L., Jacob, D. J., Liu, X., Huang, G., Li, K., Liao, H., Wang, T., 2019. An evaluation of the ability of the
536 Ozone Monitoring Instrument (OMI) to observe boundary layer ozone pollution across China: application to
537 2005–2017 ozone trends. *Atmos. Chem. Phys.* 19, 6551–6560, <https://doi.org/10.5194/acp-19-6551-2019>.

538 Shen, L., Wang, Z., Cheng, H., Liang, S., Xiang, P., Hu, K., Yin, T., Yu, J., 2020. A Spatial-Temporal Resolved
539 Validation of Source Apportionment by Measurements of Ambient VOCs in Central China, *Int. J. Env. Res. Pub.*
540 *He.* 17, 791, <https://doi.org/10.3390/ijerph17030791>.

541 Shi, J., Deng, H., Bai, Z., Kong, S., Wang, X., Hao, J., Han, X., Ning, P., 2015. Emission and profile characteristic
542 of volatile organic compounds emitted from coke production, iron smelt, heating station and power plant in
543 Liaoning Province, China. *Sci. Total Environ.* 515, 101–108.

544 Sillman, S., 1999. The relation between ozone, NO_x and hydrocarbons in urban and polluted rural environments,
545 *Atmos. Environ.*, 33, 1821–1845, 1999.

546 Sindelarova, K., Markova, J., Simpson, D., Huszar, P., Karlicky, J., Darras, S., Granier, C., 2022. High-resolution
547 biogenic global emission inventory for the time period 2000–2019 for air quality modelling. *Earth Syst. Sci. Data*.
548 14, 251–270.

549 Sinha, B.P. and Sinha, V., 2019. Source apportionment of volatile organic compounds in the northwest Indo-
550 Gangetic Plain using a positive matrix factorization model. *Atmos. Chem. Phys.* 19, 15467–15482.

551 Song, M.D., Li, X., Yang, S.D., Yu, X.A., Zhou, S.X., Yang, Y.M., Chen, S.Y., Dong, H.B., Liao, K.R., Chen,
552 Q., Lu, K.D., Zhang, N.N., Cao, J.J., Zeng, L.M., Zhang, Y.H., 2021. Spatiotemporal variation, sources, and
553 secondary transformation potential of volatile organic compounds in Xi'an, China. *Atmos. Chem. Phys.* 21,
554 4939–4958.

555 Stavrakou, T., Müller, J.-F., Bauwens, M., De Smedt, I., Van Roozendael, M., Guenther, A., Wild, M., Xia, X.,
556 2014. Isoprene emissions over Asia 1979–2012: impact of climate and land-use changes. *Atmos. Chem. Phys.*
557 14, 4587–4605, <https://doi.org/10.5194/acp-14-4587-2014>.

558 Sun, W., Wang, D., Yao, L., Fu, H., Fu, Q., Wang, H., Li, Q., Wang, L., Yang, X., Xian, A. (2019) Chemistry-
559 triggered events of PM_{2.5} explosive growth during late autumn and winter in Shanghai, China. *Environmental*
560 *pollution.* 254, 112864.

561 Sun, Y. L., He, Y., Kuang, Y., Xu, W. Y., Song, S. J., Ma, N., Tao, J. C., Cheng, P., Wu, C., Su, H., Cheng, Y. F.,
562 Xie, C. H., Chen, C., Lei, L., Qiu, Y. M., Fu, P. Q., Croteau, P., Worsnop, D. R., 2020. Chemical Differences
563 Between PM₁ and PM_{2.5} in Highly Polluted Environment and Implications in Air Pollution Studies. *Geophys.*
564 *Res. Lett.* 47, No. e2019GL086288.

565 Tsai, S. M., Zhang, J. J., Smith, K. R., Ma, Y., Rasmussen, R. A., Khalil, M. A. K., 2003. Characterization of
566 Non-methane Hydrocarbons Emitted from Various Cookstoves Used in China. *Environ. Sci. Technol.* 37, 2869–

567 2877.

568 Tong, Y., Pospisilova, V., Qi, L., Duan, J., Gu, Y., Kumar, V., Rai, P., Stefenelli, G., Wang, L., Wang, Y., Zhong,
569 H., Baltensperger, U., Cao, J., Huang, R.J., Prévôt, A. S. H., Slowik, J. G., 2021. Quantification of solid fuel
570 combustion and aqueous chemistry contributions to secondary organic aerosol during wintertime haze events in
571 Beijing. *Atmos. Chem. Phys.* 21, 9859–9886.

572 Wang, H.L., Chen, C.H., Wang, Q., Huang, C., Su, L.Y., Huang, H.Y., Lou, S.R., Zhou, M., Li, L., Qiao, L.P.,
573 Wang, Y.H., 2013a. Chemical loss of volatile organic compounds and its impact on the source analysis through
574 a two-year continuous measurement. *Atmos. Environ.* 80, 488–498.

575 Wang, M., Shao, M., Lu, S.H., Yang, Y.D., Chen, W.T., 2013b. Evidence of coal combustion contribution to
576 ambient VOCs during winter in Beijing. *Chin. Chem. Lett.* 24, 829–832.

577 Wang, J., Jin, L., Gao, J., Shi, J., Zhao, Y., Liu, S., Jin, T., Bai, Z., Wu, C.Y., 2013c. Investigation of speciated
578 VOC in gasoline vehicular exhaust under ECE and EUDC test cycles. *Sci. Total Environ.* 445, 110–116.

579 Wang, Y.S., Yao, L., Wang, L.L., Liu, Z.R., Ji, D.S., Tang, G. Q., Zhang, J.K., Sun, Y., Hu, B., Xin, J.Y., 2014a.
580 Mechanism for the formation of the January 2013 heavy haze pollution episode over central and eastern China.
581 *Sci. China Earth Sci.* 57, 14–25, <https://doi.org/10.1007/s11430-013-4773-4>.

582 Wang, H., Qiao, Y., Chen, C., Lu, J., Dai, H., Qiao, L., Lou, S., Huang, C., Li, L., Jing, S., Wu, J., 2014b. Source
583 Profiles and Chemical Reactivity of Volatile Organic Compounds from SolventUse in Shanghai, China. *Aerosol*
584 *Air Qual. Res.* 14, 301–310.

585 Wang, T., Xue, L., Brimblecombe, P., Lam, Y.F., Li, L., Zhang, L., 2017. Ozone Pollution in China: A Review
586 of Concentrations, Meteorological Influences, Chemical Precursors, and Effects. *Sci. Total Environ.* 575,
587 1582–1596.

588 Wang, J., Yang, Y., Zhang, Y., Niu, T., Jiang, X., Wang, Y., Che, H., 2019. Influence of meteorological
589 conditions on explosive increase in O₃ concentration in troposphere. *Sci.Total Environ.* 652, 1228-1241.

590 Wang, M. L., Li, S.Y., Zhu, R.C., Zhang, R.Q., Zu, L., Wang, Y.J., Bao, X.F., 2020. On-road tailpipe emission
591 characteristics and ozone formation potentials of VOCs from gasoline, diesel and liquefied petroleum gas fueled
592 vehicles. *Atmos. Environ.* 223, 117294.

593 Warneke, C., McKeen, S. A., de Gouw, J. A., Goldan, P. D., Kuster, W. C., Holloway, J. S., Williams, E. J.,
594 Lerner, B. M., Parrish, D. D., Trainer, M., Fehsenfeld, F. C., Kato, S., Atlas, E. L., Baker, A., Blake, D. R., 2007.
595 Determination of urban volatile organic compound emission ratios and comparison with an emissions database.
596 *J. Geophys. Res.* 112, D10S47, <https://doi.org/10.1029/2006jd007930>.

597 Wu, R.R., Li, J., Hao, Y.F., Li, Y.Q., Zeng, L.M., Xie, S.D., 2016. Evolution process and sources of ambient
598 volatile organic compounds during a severe haze event in Beijing, China. *Sci. Total. Environ.* 560-561, 62-72.

599 Wu, R. and Xie, S., 2018. Spatial Distribution of Secondary Organic Aerosol Formation Potential in China
600 Derived from Speciated Anthropogenic Volatile Organic Compound Emissions, *Environ. Sci. Technol.* 52,
601 8146–8156, <https://doi.org/10.1021/acs.est.8b01269>.

602 Xing, J., Wang, S. X., Jang, C., Zhu, Y., Hao, J. M., 2011. Nonlinear response of ozone to precursor emission
603 changes in China: a modeling study using response surface methodology. *Atmos. Chem. Phys.* 11, 5027–5044.

604 Xu, W., Sun, Y., Wang, Q., Zhao, J., Wang, J., Ge, X., Xie, C., Zhou, W., Du, W., Li, J., Fu, P., Wang, Z., Worsnop,
605 D.R., Coe, H., 2019. Changes in Aerosol Chemistry From 2014 to 2016 in Winter in Beijing: Insights From High-
606 Resolution Aerosol Mass Spectrometry. *J. Geophys. Res.: Atmos.* 124 (2), 1132–1147

607 Xu, Q., Wang, S., Jiang, J., 2019. Nitrate dominates the chemical composition of PM_{2.5} during haze event in
608 Beijing, China. *Sci. Total. Environ.* 689:1293-1303.

609 Xue, Y., Ho, S. S. H., Huang, Y., Li, B., Wang, L., Dai, W., Cao, J., Lee, S., 2017. Source apportionment of
610 VOCs and their impacts on surface ozone in an industry city of Baoji, Northwestern China. *Sci. Rep.* 7, 9979,
611 <https://doi.org/10.1038/s41598-017-10631-4>.

612 Xue, T., Zheng, Y., Geng, G., Xiao, Q., Meng, X., Wang, M., Li, X., Wu, N., Zhang, Q., Zhu, T., 2020a.
613 Estimating Spatiotemporal Variation in Ambient Ozone Exposure during 2013–2017 Using a Data-Fusion Model.
614 *Environ Sci. Technol.* 54, 14877–14888.

615 Xue, Y., Huang, Y., Ho, S.S.H., Chen, L., Wang, L., Lee, S., Cao, J., 2020b. Origin and transformation of ambient
616 volatile organic compounds during a dust-to-haze episode in northwest China. *Atmos. Chem. Phys.* 20, 5425–
617 5436.

618 Yan, Y., Peng, L., Li, R., Li, Y., Li, L., Bai, H., 2017. Concentration, ozone formation potential and source analysis
619 of volatile organic compounds (VOCs) in a thermal power station centralized area: A study in Shuozhou, China.
620 *Environ. Pollut.* 223, 295–304.

621 Yang, W.Q., Zhang, Y.L., Wang, X.M., Li, S., Zhu, M., Yu, Q.Q., Li, G.H., Huang, Z.H., Zhang, H.N., Wu, Z.F.,
622 Song, W., Tan, J.H., Shao, M., 2018. Volatile organic compounds at a rural site in Beijing: influence of temporary
623 emission control and wintertime heating. *Atmos. Chem. Phys.* 18, 12663–12682.

624 Yao, Y.C., Tsai, J.H., Wang, I.T., 2013. Emissions of gaseous pollutant from motorcycle powered by ethanol-
625 gasoline blend. *Appl. Energy.* 102, 93–100.

626 Yao, Z., Wu, B., Shen, X., Cao, X., Jiang, X., Ye, Y., He, K., 2015. On-road emission characteristics of VOCs from
627 rural vehicles and their ozone formation potential in Beijing, China. *Atmos. Environ.* 105, 91–96.

628 Yao, L., Wang, D., Fu, Q., Qiao, L., Wang, H., Li, L., Sun, W., Li, Q., Wang, L., Yang, X., 2019. The effects of
629 firework regulation on air quality and public health during the Chinese Spring Festival from 2013 to 2017 in a

630 Chinese megacity. *Environ Int.* 126, 96-106.

631 Yuan, B., Shao, M., Lu, S., Wang, B., 2010. Source profiles of volatile organic compounds associated with solvent
632 use in Beijing, China. *Atmos. Environ.* 44, 1919–1926.

633 Zhai, S., Jacob, D.J., Wang, X., Shen, L., Li, K., Zhang, Y., Gui, K., Zhao, T., Liao, H., 2019. Fine particulate
634 matter (PM_{2.5}) trends in China, 2013–2018: separating contributions from anthropogenic emissions and
635 meteorology, *Atmos. Chem. Phys.* 19, 11031– 11041, <https://doi.org/10.5194/acp-19-11031-2019>.

636 Zhang, Y., Wang, X., Zhang, Z., Lu, S., Shao, M., Lee, F.S. C., Yu, J., 2013. Species profiles and normalized re
637 activity of volatile organic compounds from gasoline evaporation in China. *Atmos. Environ.* 79, 110–118.

638 Zhang, X., Xue, Z., Li, H., Yan, L., Yang, Y., Wang, Y., Duan, J., Li, L., Chai, F., Cheng, M., Zhang, W., 2017.
639 Ambient volatile organic compounds pollution in China. *J Environ. Sci.* 55, 69-75, 10.1016/j.jes.2016.05.036.

640 Zhang, Y., Li, R., Fu, H., Zhou, D., Chen, J., 2018. Observation and analysis of atmospheric volatile organic
641 compounds in a typical petrochemical area in Yangtze River Delta, China. *J. Environ. Sci.* 71, 233-248.

642 Zhao, D., Liu, G., Xin, J., Quan, J., Wang, Y., Wang, X., 2020. Haze pollution under a high atmospheric
643 oxidization capacity in summer in Beijing: insights into formation mechanism of atmospheric physicochemical
644 processes. *Atmos. Chem. Phys.* 20, 4575-4592.

645 Zhao, Q.Y., Bi, J., Liu, Q., Ling, Z.H., Shen, G.F., Chen, F., Qiao, Y.Z., Li, C.Y., Ma, Z.W., 2020. Sources of
646 volatile organic compounds and policy implications for regional ozone pollution control in an urban location of
647 Nanjing, East China. *Atmos. Chem. Phys.* 20, 3905–3919.

648 Zheng, J., Yu, Y., Mo, Z., Zhang, Z., Wang, X., Yin, S., Peng, K., Yang, Y., Feng, X., Cai, H., 2013. Industrial
649 sector-based volatile organic compound (VOC) source profiles measured in manufacturing facilities in the Pearl
650 River Delta, China. *Sci. Total Environ.* 456, 127–136.

651 Zheng, H., Kong, S., Xing, X., Mao, Y., Hu, T., Ding, Y., Li, G., Liu, D., Li, S., Qi, S., 2018. Monitoring of
652 volatile organic compounds (VOCs) from an oil and gas station in northwest China for 1 year. *Atmos. Chem.*
653 *Phys.* 18, 4567-4595.
654

Figure captions

656 **Figure 1.** Time series of meteorological parameters and levels of air pollutants during the sampling
657 period.

658 **Figure 2.** Comparison of the concentration and composition of major chemical groups observed in
 659 2019 (this study), 2016 (Liu et al., 2020) and 2014 (Li et al., 2015).

660 **Figure 3.** Comparison of major meteorological parameters and air pollutants on clean and polluted
661 days. The averaged levels of temperature (T), wind speed (WS), and O₃ and NO_x concentrations on
662 (a) O₃ compliance during the O₃-polluted months, (b) O₃ pollution days during the O₃-polluted
663 months, and (c) differences in VOCs mixing ratios between O₃ compliance and pollution days. The
664 averaged levels of temperature (T), wind speed (WS), relative humidity (RH), and PM_{2.5}
665 concentrations on (d) PM_{2.5} compliance during the PM_{2.5}-polluted months, (e) PM_{2.5} pollution days
666 during the PM_{2.5}-polluted months, and (f) differences in VOCs mixing ratios between PM_{2.5}
667 compliance and pollution days.

668 **Figure 4.** Statistic decomposition of meteorological and emission contribution to O₃ and PM_{2.5}
669 levels during different periods.

670 **Figure 5.** OFP and SOAOFP by chemical groups during different periods.

671 **Figure 6.** Ratios of i/n-pentane and toluene/benzene at different $PM_{2.5}$ and O_3 levels.

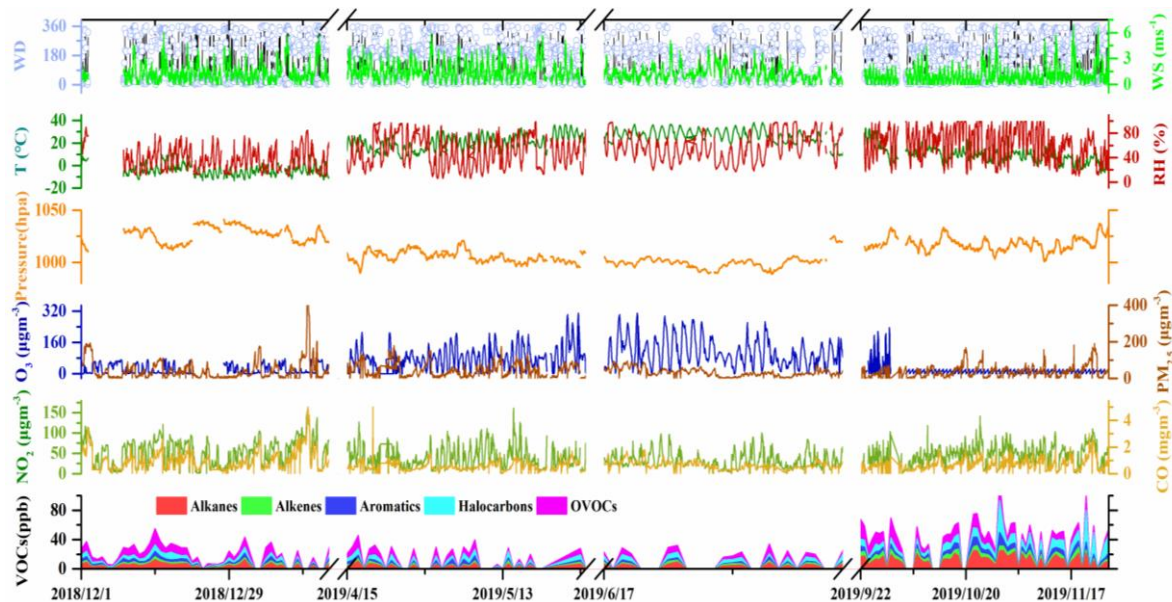
672 **Figure 7.** Source profiles of VOCs identified using the PMF model and the relative contributions of
673 the individual VOC species.

674 **Figure 8.** Contributions of each source to VOCs on (a) O₃ compliance days during the O₃-polluted
675 months, (b) O₃ pollution days during the O₃-polluted months, and during (c) the non-O₃-polluted
676 months. Contributions of each source to VOCs on (d) PM_{2.5} compliance days during the PM_{2.5}-

677 polluted months, (e) PM_{2.5} pollution days during the PM_{2.5}-polluted months, and (f) during the non-
678 PM_{2.5}-polluted months, during different periods.

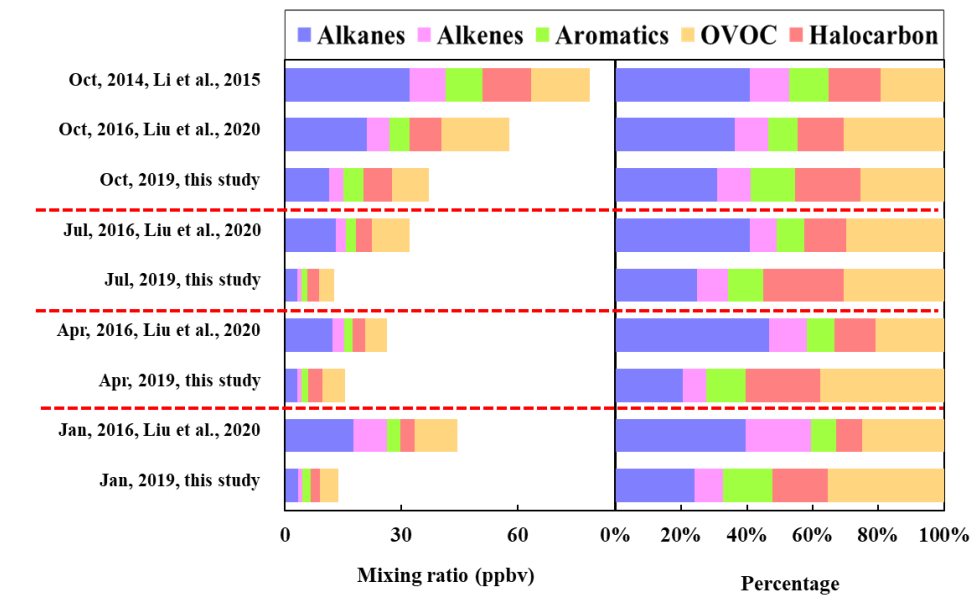
679 **Figure 9.** Contributions of each source to OFP and SOAFP during different periods.

680 **Figure 10.** OFP values of the dominant VOC species in the different source categories for the O₃
681 pollution (a) and compliance (b) days of the O₃-polluted months, and SOAFP values for the PM_{2.5}
682 pollution (c) and compliance (d) days of the PM_{2.5}-polluted months.

Fig. 1.

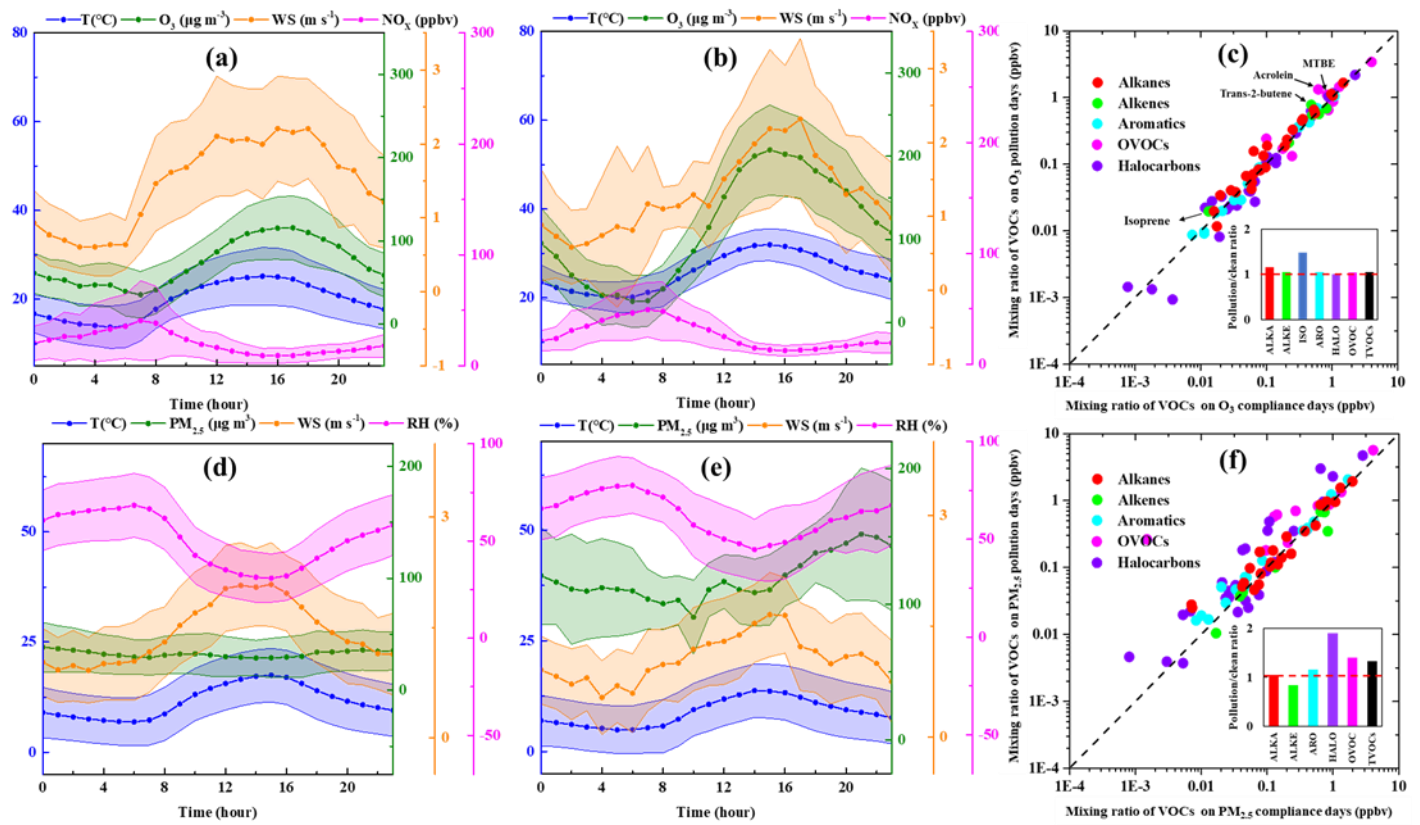
686

687

688 **Figure 2.**

689

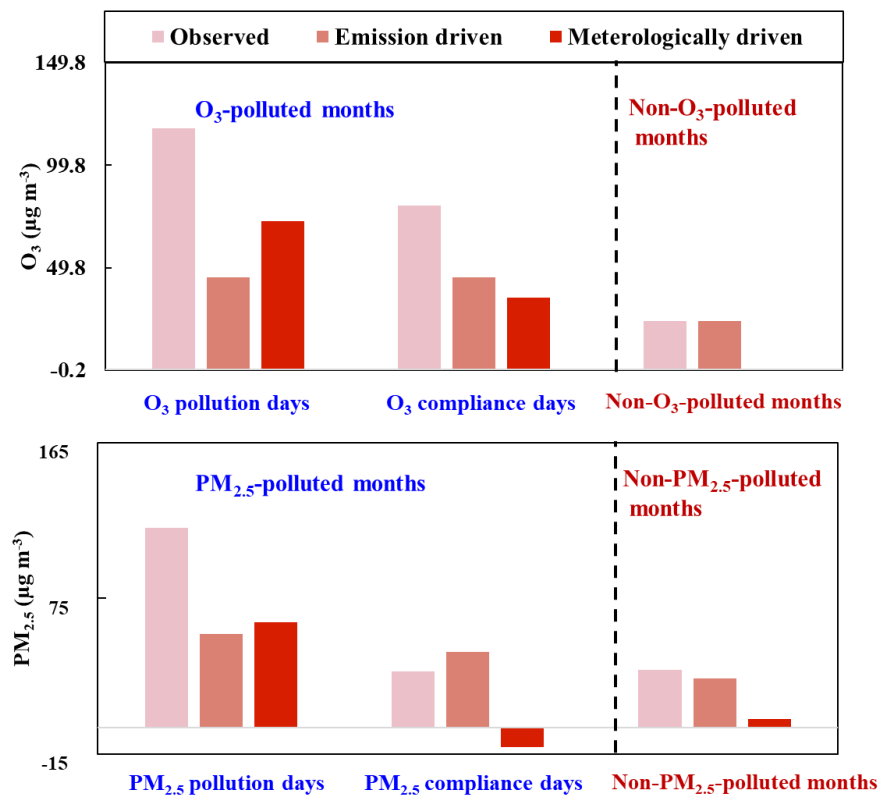
690

Fig. 3.

694 **Fig. 4**

695

696



697

Fig. 5

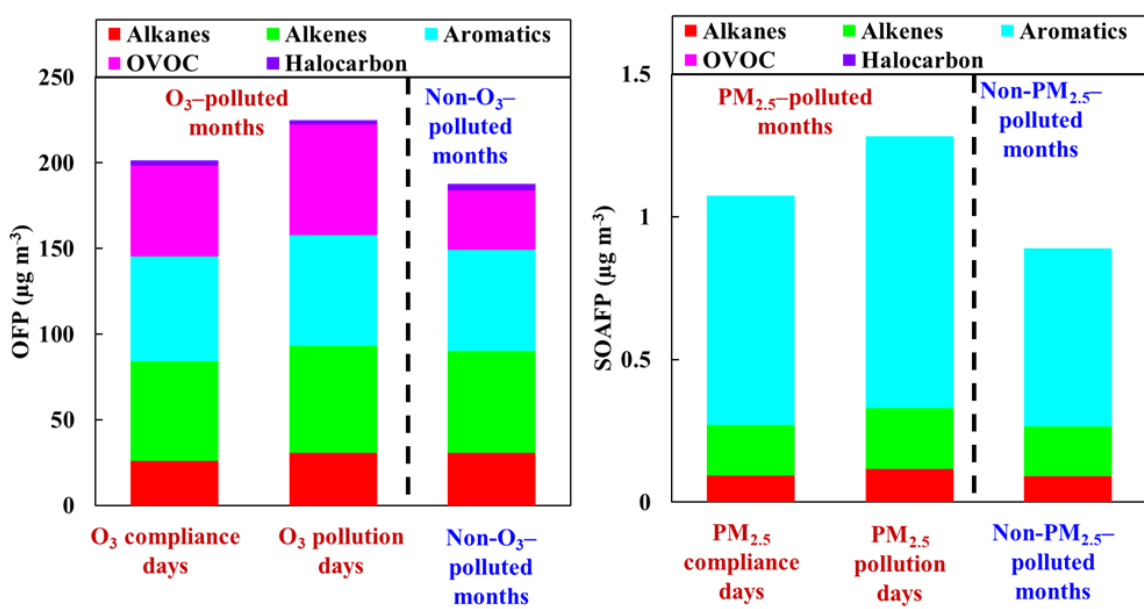


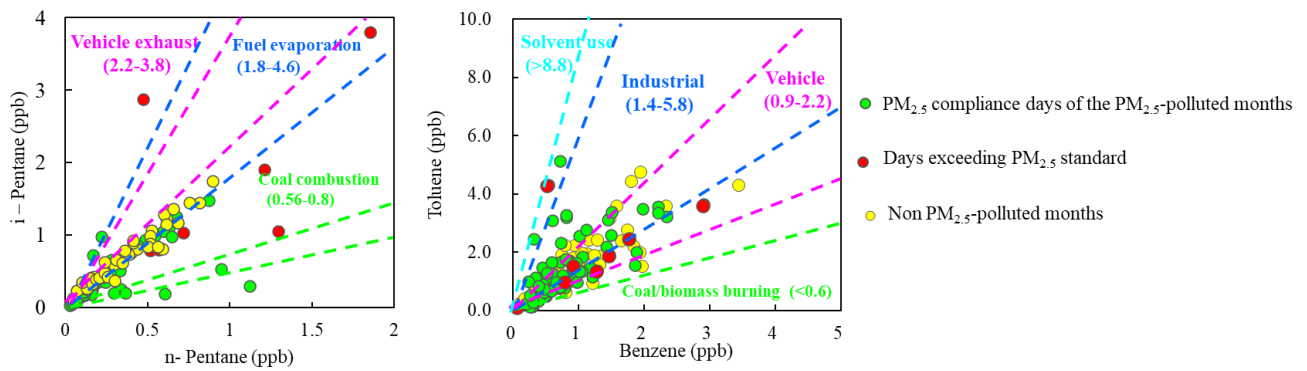
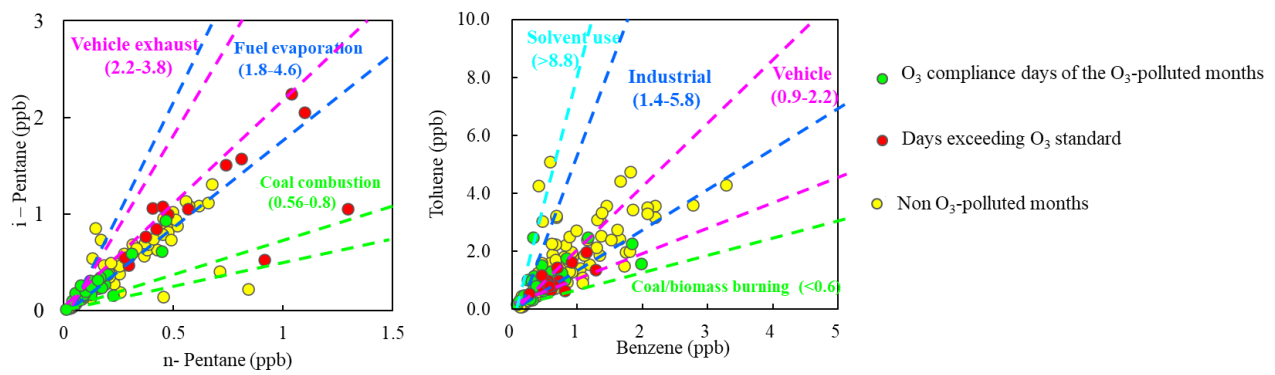
Fig. 6**Ratios of i/n-pentane and toluene/benzene at different PM_{2.5} levels****Ratios of i/n-pentane and toluene/benzene at different O₃ levels**

Fig. 7.

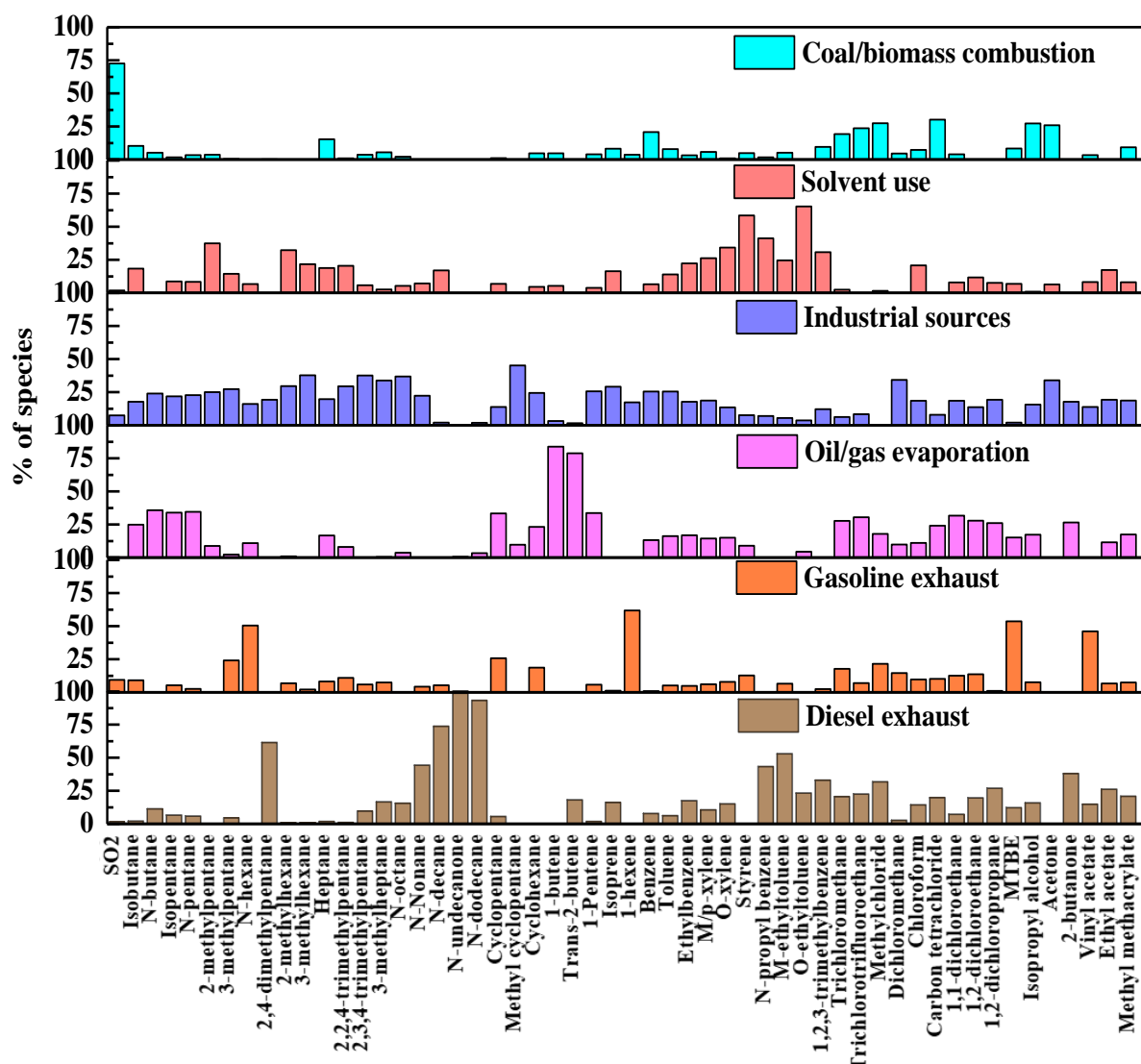


Fig. 8

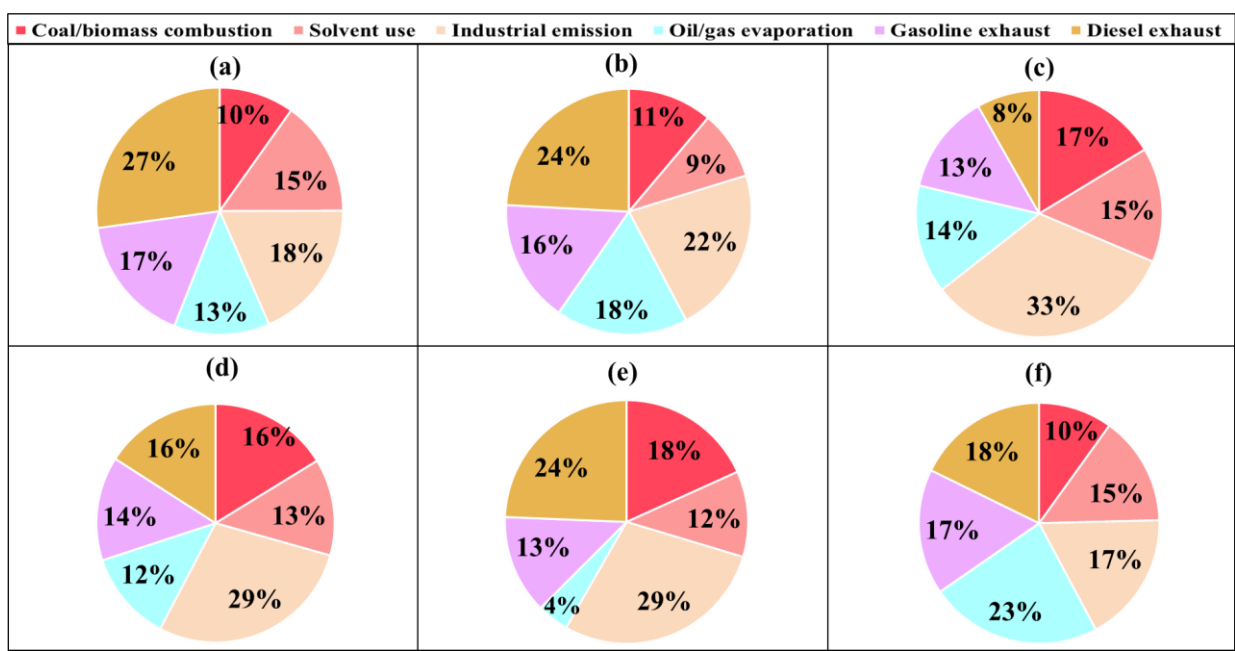


Fig. 9

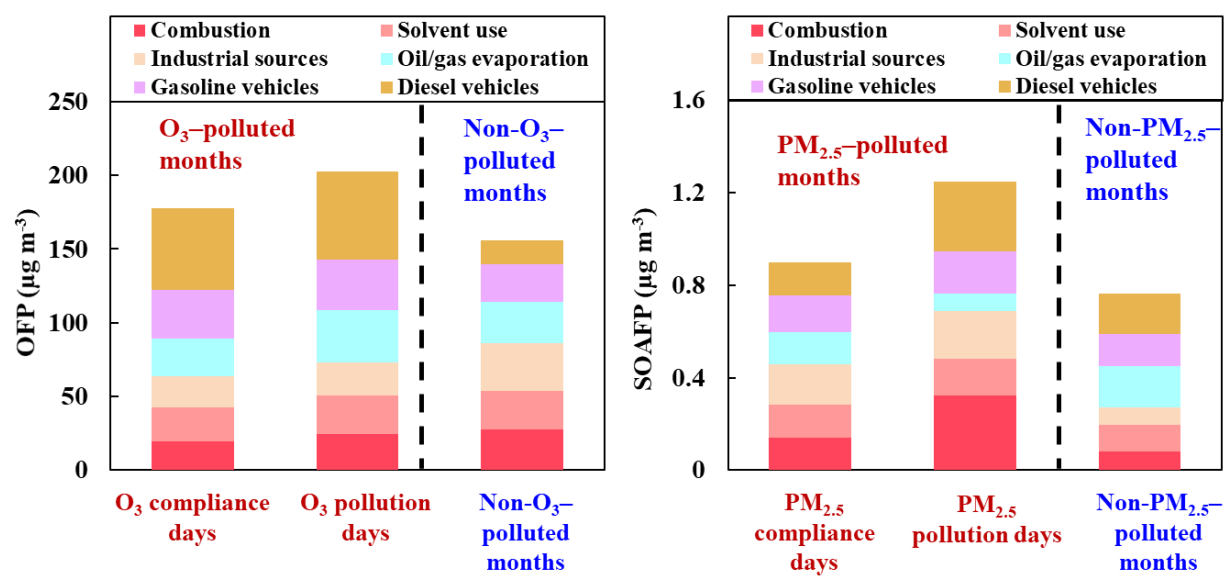


Fig. 10

